Chinese Chemical Letters 33 (2022) 807–811

Contents lists available at ScienceDirect

Chinese Chemical Letters

journal homepage: www.elsevier.com/locate/cclet

High-performance cascade nanoreactor based on halloysite nanotubes-integrated enzyme-nanozyme microsystem

Yan Liu[a], Rui Lv[a], Shiyong Sun[a,*], Daoyong Tan[a], Faqin Dong[a], Yevgeny A. Golubev[b], Xiaoqin Nie[a], Olga B. Kotova[b], Jin Liu[a], Ke Wang[a]

[a] School of Environment and Resource, Key Laboratory of Solid Waste Treatment and Resource Recycle of Ministry of Education, Southwest University of Science and Technology, Mianyang 621010, China
[b] Yushkin's Institute of Geology, Komi Science Center, Ural Branch of RAS, ul. Pervomayskaya, 54, Syktyvkar 167982, Russia

ARTICLE INFO

Article history:
Received 21 May 2021
Revised 17 June 2021
Accepted 30 June 2021
Available online 7 July 2021

Keywords:
Halloysite nanotubes
Fe-aminoclay
Nanozyme
Cascade nanoreactor
Catalysis enhancement

ABSTRACT

Various enzymatic reactions or enzymatic cascade reactions occur efficiently in biological microsystems due to space constraints or orderly transfer of intermediate products. Inspired by this, the horseradish peroxidase (HRP)-like nanozyme (Fe-aminoclay) was *in situ* synthesized on the surface of alkali-activated halloysite nanotubes and the natural enzyme (glucose oxidase, GOx) was immobilized on it to construct a high-efficiency GOx-FeAC@AHNTs cascade nanoreactor. In which, FeAC@AHNTs can not only be used as a carrier for immobilized enzymes, but also help its catalytic activity to cooperate with glucose oxidase in a cascade reaction. The microcompartments and substrate channel effect of this enzyme-nanozyme microsystem exhibit a superior catalytic performance than that of natural enzyme system, and exhibits excellent long-term stability and recyclability. Subsequently, the GOx-FeAC@AHNTs cascade nanoreactor was employed as a glucose colorimetric platform, which displayed a low detection limit (0.47 μmol/L) in glucose detection. This enzyme-nanoenzyme nanoreactor provides a simple and effective example for constructing a multi-enzyme system with limited space, and lays the foundation for subsequent research in the fields of biological analysis and catalysis.

© 2021 Published by Elsevier B.V. on behalf of Chinese Chemical Society and Institute of Materia Medica, Chinese Academy of Medical Sciences.

The various delicate biochemical processes performed in organisms require joint participation and coordination between multiple-enzymes, including during protein synthesis, signal transduction and metabolism [1]. These enzymes perform multi-step or cascade reactions under space constraints (microcompartments) and in substrate-channeling environments, which can greatly increase overall activity and help maintain the efficiency and order of metabolic processes [2,3]. Inspired by biological microsystems, many scientists have tried to construct efficient cascade enzymatic microsystems similar to those *in vivo* [4,5]. However, *in vitro* multi-enzyme cascade reaction systems in free solution states are limited by difficult product recovery and poor stability. As a result, current research focuses on constructing multi-enzyme microsystems *in vitro via* co-localizing enzymes on suitable supports, carriers or assembly enzymes [6]. Multi-enzyme immobilization is regarded as a promising route to substrate channelization with the advantages of less operation in the reaction process, small reactor volume and easy storage [6]. This co-immobilization strategy places the active sites of the enzymes close to each other, reduces the mass transfer distance between the enzymes, enhances the local interoperability and efficiency of the catalytic reaction, and improves the stability and reusability [5,7].

To date, there have been many strategies for the immobilization of multiple-enzymes, including microencapsulation [8], layer-by-layer self-assembly [7,9] and covalent bonding [10,11]. Due to the advantages of nanozymes, such as their high specific surface area, high stability, strong operability and low cost compared with natural enzymes, many scientists are focusing on the construction of enzyme-nanozyme microsystem inside nanostructures to integrate the advantages of both nanozymes and immobilization [3,12]. CeO_2 with peroxidase-like activity and glucose oxidase (GOx) have been sealed together by self-assembly to form a hybrid nanozyme complex (CeO_2/GOx) [13]. Porphyrin iron with horseradish peroxidase (HRP)-like catalytic properties has been co-embedded with GOx in a hydrogel network to construct a GOx-porphyrin iron enzyme-nanozyme cascade system [14].

Synthetic aminopropyl-functionalized iron phyllosilicate clay (Fe-aminoclay, FeAC) exhibits HRP-like activity [15,16]. It has exhibit a 1:1 dioctahedral phyllosilicate structure, which can be exfoliated into monoliths *via* the protonation of its amino groups in water and restored to a stacked state in a less polar solvent

* Corresponding author.
E-mail address: shysun@swust.edu.cn (S. Sun).

https://doi.org/10.1016/j.cclet.2021.06.087
1001-8417/© 2021 Published by Elsevier B.V. on behalf of Chinese Chemical Society and Institute of Materia Medica, Chinese Academy of Medical Sciences.

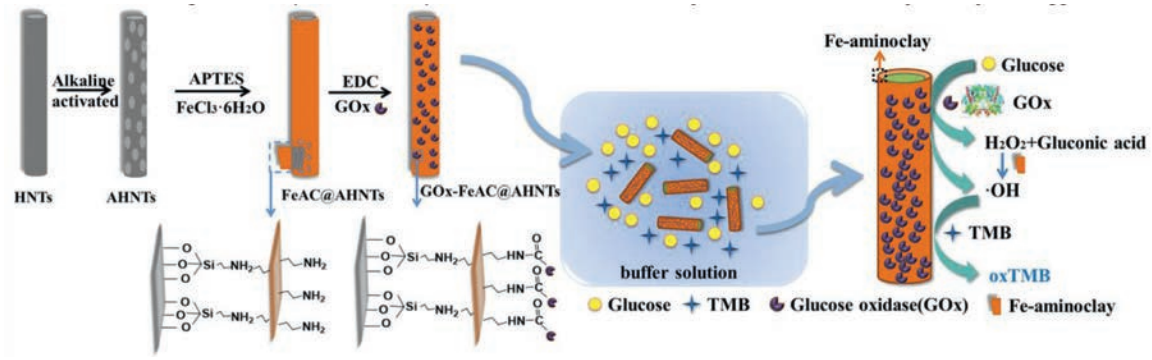

Scheme 1. Schematic illustration of the cascade microsystem of alkali activated halloysite nanotubes (AHNTs) integrated Fe-aminoclay (FeAC) and glucose oxidase (GOx).

such as ethanol [17]. Additionally, the exfoliated FeAC monoliths can strongly interact with biomolecules (*i.e.*, DNA, lipids and proteins) and can be used to prepare highly stable functionalized nano–bio hybrid materials [18]. Furthermore, halloysite is a natural clay mineral composed of alternating layers of silica and alumina geologically rolled into mesoporous tubular particles, which exhibit positive and negative charges on inner and outer surface in a wide pH range (pH 2–8), respectively [19]. It has been considered halloysite nanotubes (HNTs) as a promising complementary platform for integrating enzyme-nanozyme microsystems. It allows FeAC with high water dispersibility and high density of positive charge–NH_3^+ groups to grow accurately *in situ* to its outer surface, due to their unique charge characteristics, large specific surface area and the permanent negative charges on their outer surfaces [19,20].

Therefore, in the present work, HNTs were selected as an excellent platform to provide a substrate-channeling environments for the chemical cascade reaction. Based on previous studies, GOx directly catalyzes glucose into gluconic acid and H_2O_2, and then the generated H_2O_2 is activated by peroxidase (such as HRP) or nanozyme with peroxidase-like activity to produce ·OH [21]. Therefore, the *in situ* synthesis of FeAC and the immobilization of GOx on HNTs are achieved through electrostatic attraction and covalent bonding, which shortens the distance between the active sites of the reaction, protects unstable intermediate products, and improve the overall activity and stability of an integrated GOx-FeAC@AHNTs microsystem. Firstly, FeAC was synthesized *in-situ* on the surface of the alkali-activated halloysite nanotubes (AHNTs) to obtain FeAC@AHNTs. GOx was then covalently attached to obtain a GOx-FeAC@AHNTs microsystem (Scheme 1). Finally, the system was employed to visually detect glucose with an extremly low detection limit. This method will pave the way for multi-enzyme immobilization and biological colorimetric sensing, among other applications.

The HNTs were previously activated with alkali to obtain AHNTs to increase their specific surface area and the amount of surface hydroxyl groups. In the ethanol/water system, hydrolysed (3-aminopropyl)triethoxysilane (APTES) was directly condensed with the hydroxyl groups on the AHNTs, thus, the amino group on APTES was modified to the surface of the AHNTs [22]. Subsequently, $FeCl_3{\cdot}6H_2O$ was added, and the Si-O bond on APTES coordinated with iron to form FeAC, thereby forming FeAC *in situ* on the AHNTs. Then, GOx was immobilized on the FeAC@AHNTs by the crosslinking agent 1-ethyl-3-(3-dimethylaminopropyl)carbodiimide hydrochloride (EDC) to obtain the GOx-FeAC@AHNTs microsystem (Scheme 1).

Scanning and transmission electron microscopy (SEM and TEM) observations showed that the tubular structures of the HNTs were maintained, but their smooth outer surface were made rough by the alkali treatment (Figs. 1a and b). Obvious adhesion aggregation was also visible on their surfaces after *in-situ* FeAC formation, and surface roughness further increased after the fixing of GOx (Fig. 1c, and Figs. S1f and h in Supporting information). Energy spectrum (EDX) and element mapping analysis also showed that the AHNTs contained essential the elements of FeAC (Figs. 1d and e). The N_2 adsorption-desorption isotherms of the AHNTs and GOx-FeAC@AHNTs exhibited the characteristics of type IV isotherms, indicating that the mesoporous nanostructures of the HNTs were activated, and the hysteresis loops of it are of type H3 as shown in Fig. S1c (Supporting information). This result corresponds to the cylindrical pores, which further shows that the HNTs retain their tubular structures after alkali activation and the subsequent load of FeAC and GOx. Brunauer-Emmett-Teller (BET) analysis showed that the specific surface areas of the HNTs and AHNTs were 39.014 and 43.491 m^3/g, respectively, indicating that the surface areas of the HNTs increased slightly after alkali activation. The average particle sizes of HNTs, AHNTs, FeAC@AHNTs and GOx-FeAC@AHNTs were 6.9, 4.8, 20 and 25 nm (Fig. S1d in Supporting information), respectively, indicating that particle size gradually increased with

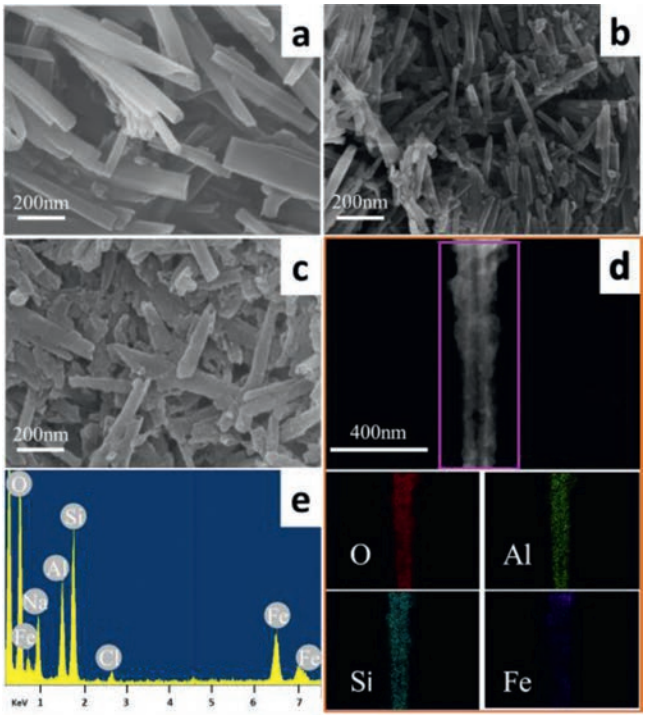

Fig. 1. SEM images of (a) natural HNTs, (b) FeAC@AHNTs and (c) GOx-FeAC@AHNTs; (d) TEM and elemental mapping images of GOx-FeAC@AHNTs; (e) EDX spectrum of GOx-FeAC@AHNTs.

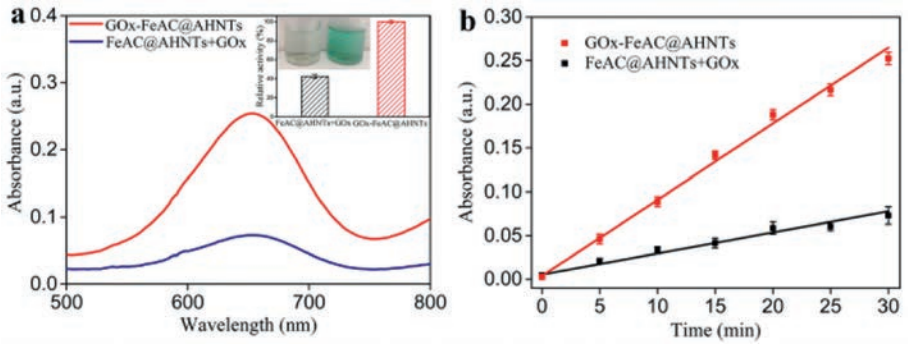

Fig. 2. (a) UV–visible spectra of the cascade reaction of free enzyme (FeAC@AHNTs + GOx) and immobilized enzyme (GOx-FeAC@AHNTs) in 0.1 mol/L NaAC-AC buffer, and cascade reaction enzyme activity of FeAC@AHNTs + GOx and GOx-FeAC@AHNTs; (b) Time absorption curve of FeAC@AHNTs + GOx and GOx-FeAC@AHNTs in 10 mmol/L glucose.

the *in-situ* immobilization of FeAC and GOx. Zeta potential analysis showed that due to the high density of positively charged $-NH_3^+$ groups on the FeAC surface, when FeAC was synthesized *in situ* on the AHNTs, the initial negative charge of −38.5 mV (AHNTs) changed to 32.3 mV (FeAC@HNTs) (Fig. S1d). Since the isoelectric point of GOx is 4.2, indicating a negative charge in aqueous media, the measured zeta potential of GOx-FeAC@HNTs is 28.8 mV, which is lower than that of FeAC@HNTs (Fig. S1d). In addition, Fourier-transform infrared spectroscopy (FT-IR) confirmed the successful grafting of APTES to the surfaces of the ANHTs, showing new characteristic vibration peaks, namely, N–H stretching and bending peaks at 3434 and 1516 cm^{-1}, and a C–H stretching peak at 1404 cm^{-1}, the stretching vibration peak at 1542 cm^{-1} of the amide II bond (C=O) is observed in GOx@FeAC@AHNTs, but absent in FeAC@AHNTs, which indicates the existence of GOx in the composite (Fig. S1b in Supporting information). X-ray diffraction (XRD) analysis showed that the typical diffraction peak of FeAC layered organoclay appeared at $2\theta = 4.71°$ after FeAC was formed *in situ* and the fixation of GOx did not change the structure of FeAC@AHNTs (Fig. S1a in Supporting information). Based on the above results, it can be inferred that the GOx-FeAC@AHNTs microsystem has been successfully constructed.

We first investigated the effects of different molar ratios of APTES and $FeCl_3{\cdot}6H_2O$ on the subsequent glucose oxidase loading and catalytic performance of the cascade reaction, and chose a molar ratio of 1:1 for subsequent experiments (Fig. S2 in Supporting information). The peroxidase activity of FeAC@AHNTs was investigated in a reaction system containing FeAC@AHNTs, H_2O_2 and 3,3′,5,5′-tetramethylbenzidine (TMB). TMB was oxidized to blue-colored oxTMB in the presence of ·OH. Controversially, the system showed a negligible color change in the absence of H_2O_2 or FeAC@AHNTs (Fig. S3a in Supporting information). A reasonable explanation may be that Fe(III) is abundant in the FeAC@AHNTs, and H_2O_2, which was activated by the FeAC, produced ·OH, which converted TMB into blue-colored oxTMB. To verify the existence of ·OH in this process, isopropanol was employed as a probe to capture it. Isopropanol was added to the above-mentioned color-developing system, and its absorption intensity was observed at 655 nm. The addition of isopropanol decreased the absorbance of the system and the reduced the intensity of the blue color (Fig. S3b in Supporting information), indicating that the FeAC@AHNTs oxidize TMB by oxidizing H_2O_2 to produce ·OH with peroxidase-like activity.

In order to evaluate the cascade performance of GOx-FeAC@AHNTs, a physical mixture of FeAC@AHNTs and GOx was used for comparison. The color intensity produced by GOx-FeAC@AHNTs was obviously deeper than that produced by physically mixed FeAC@AHNTs + GOx, the absorbance was 3.5 times greater, the relative activity of enzyme catalysis was 2.33 times greater (Fig. 2a), and the reaction velocity of the GOx-FeAC@AHNTs microsystem was significantly faster than that of the FeAC@AHNTs + GOx system within 30 min (Fig. 2b), indicating that GOx chemically bonds with FeAC@AHNTs in the GOx-FeAC@AHNTs microsystem and improves the performance of the enzyme cascade.

Subsequently, the catalytic stability of GOx-FeAC@AHNTs was investigated under different environmental conditions (pH and temperature) and compared with that of the natural enzyme system (GOx + HRP). GOx-FeAC@AHNTs and GOx + HRP were incubated at various pH and temperature conditions for 6 h and 30 min, respectively. The results showed that the GOx-FeAC@AHNTs system has a higher acid-base tolerance, while GOx + HRP showed significantly less catalytic stability. At temperatures of 30–90 °C, GOx-FeAC@AHNTs were more stable, while the activity of GOx + HRP was sharply reduced at temperature above 50 °C (Figs. 3a and b). In addition, GOx-FeAC@AHNTs had better storage stability and reusability. After 7 repeated uses of the GOx-FeAC@AHNTs system, enzyme activity was still approximately 60%, and the relative activity of GOx-FeAC@AHNTs was approximately 65% after 20 days of storage at 4 °C (Figs. 3c and d). Subsequently, the sample was recovered 7 times, its micromorphology wasn't distinctive changed based on the SEM and TEM observations (Figs. S1g–j in Supporting information). Furthermore, there are also no significant changes based on the XRD patterns and FT-IR spectra (Figs. S1a and b in Supporting information). It seems that the inevitably loss of samples led to a decrease in catalytic activity during the recovery processes such as centrifugation and washing. The kinetic parameters also show that the K_m (51.78 and 53.62) of GOx-FeAC@AHNTs for different substrates (glucose and TMB, respectively) were larger than those of GOx + HRP (2.13 and 0.59 for glucose and TMB, respectively) (Table S1 in Supporting information). Due to the presence of the HNTs sterically hindering GOx, the affinity of the GOx-FeAC@AHNTs system for its substrate is poorer than that of the natural enzyme system, but its maximum reaction velocity Vmax (5.84 and 11.6 for glucose and TMB, respectively) is greater than that of the natural enzyme system (0.17 and 0.18 for glucose and TMB, respectively) (Table S1). The velocity of a cascade reaction depends on the consumption of the substrate and accumulation of the product in the pores of the carrier and is improved by eliminating lag time [5]. Therefore, the fixation successively of FeAC and GOx in the mesoporous HNTs has greatly shortened the distance between the substrates. The H_2O_2 formed *in situ* will immediately react with the adjacent FeAC@AHNTs to minimize the diffusion and self-decomposition of H_2O_2, eliminate accumulation of intermediate products, thereby obtaining higher catalytic performance.

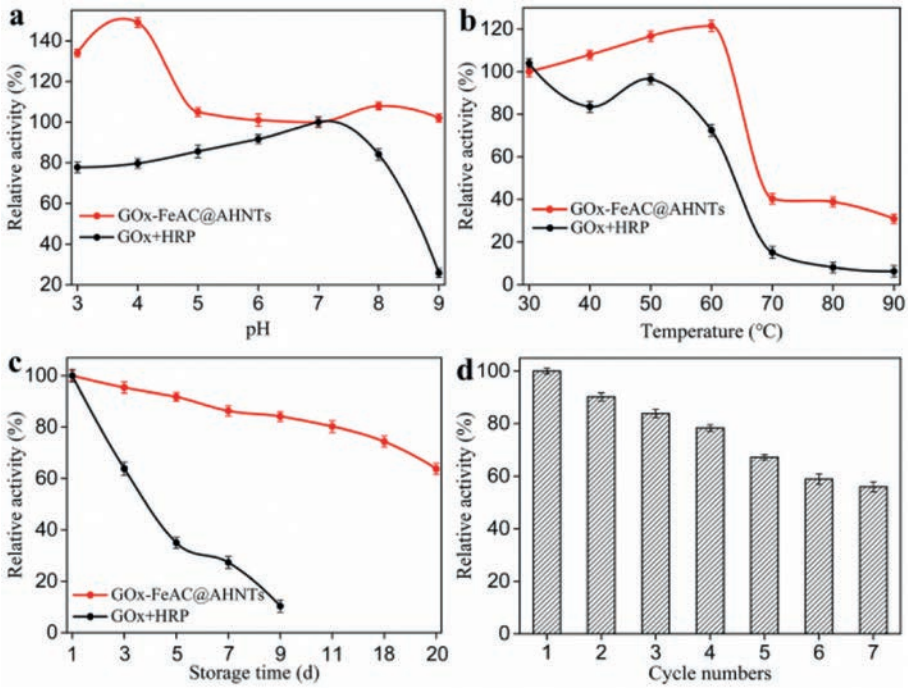

Fig. 3. The catalytic stability of GOx-FeAC@AHNTs and GOx + HRP systems. The pH stability (a), temperature stability (b), storage stability (c) and recyclability (d) of GOx-FeAC@AHNTs and GOx + HRP.

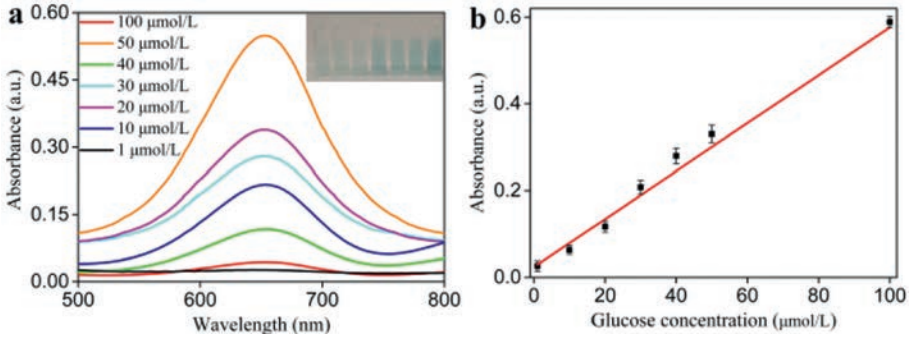

Fig. 4. (a) UV–vis spectra and digital photo (inset) of cascade reaction with the glucose concentration from 1 μmol/L to 100 μmol/L and (b) linear calibration curve for glucose detection at 655 nm.

Table 1
The comparison of different types of nanozymes for Colorimetric assay of glucose.

Colorimetric system	Liner range (μmol/L)	LOD (μmol/L)	Reference
GOx/BSA-PtNP@$MnCo_2O_4$	10–120	8.1	[23]
Au-50@TiO_2	5–100	4	[24]
2.6Pt/EMT	2.9–29.4	1.1	[25]
GOD@Cu-hemin MOF	10–1000	2.8	[26]
GOx-FeAC@AHNTs	1–100	0.47	This work

Finally, the enzymatic cascade performance of GOx-FeAC@AHNTs was further investigated *via* the detection of glucose using TMB as a chromogenic substrate. Various concentrations of glucose were added into the color-developing GOx-FeAC@AHNTs microsystem. As the amount of glucose increased, the color of the solution darkened, with a linear relationship from 1 μmol/L to 100 μmol/L glucose (R^2 = 0.9912) (Figs. 4a and b). The limit of detection (LOD) for detecting glucose was 0.47 μmol/L. Compared with other systems, this method has an extremely high sensitivity in detecting glucose (Table 1).

In conclusion, a promising cascade microsystem was constructed with a natural enzyme (GOx) and nanozyme (FeAC) co-immobilized on AHNTs, in which GOx oxidizes glucose to produce H_2O_2, then H_2O_2 is quickly catalyzed by the adjacent FeAC to produce $^{\cdot}OH$, which can oxidize TMB into blue-colored oxTMB. Due to the microcompartment restriction and substrate-channeling effects, the diffusion of enzyme intermediates is minimized, thereby improving the overall efficiency of the cascade reaction. The GOx-FeAC@AHNTs microsystem offers excellent catalytic efficiency and recyclability as well as strong resistance to high temperatures and harsh pH conditions compared to the free enzyme and nanozyme system. The established strategy provides a promising cascade platform for constructing enzyme-nanozyme microsystems.

Declaration of competing interest

The authors declare that they have no known competing financial interests or personal relationships that could have appeared to influence the work reported in this paper.

Acknowledgments

This work was supported by the National Natural Science Foundation of China (NSFC, Nos. 42061134018, 42011530085 and

41877323), the Russian Science Foundation (RSF, No. 21-47-00019, Russia), the Sichuan Science and Technology Program (No. 2019JDJQ0056, China).

Appendix A. Supplementary data

Supplementary material associated with this article can be found, in the online version, at doi:10.1016/j.cclet.2021.06.087.

References

[1] S. Schoffelen, J.C.M. van Hest, Soft Matter 8 (2012) 1736–1746.
[2] N. Liu, Z. Yang, X. Lou, et al., Anal. Chem. 87 (2015) 4037–4041.
[3] X. Cheng, Z. Zheng, X. Zhou, Q. Kuang, ACS Sustain. Chem. Eng. 8 (2020) 17783–17790.
[4] K. Zhou, T. Tian, C. Wang, et al., J. Am. Chem. Soc. 142 (2020) 20605–20615.
[5] E.T. Hwang, S. Lee, ACS Catal. 9 (2019) 4402–4425.
[6] S. Ren, C. Li, X. Jiao, et al., Chem. Eng. J. 373 (2019) 1254–1278.
[7] J. Yin, T. Xu, N. Zhang, H. Wang, Anal. Chem. 88 (2016) 7730–7737.
[8] R. Lv, S. Lin, S. Sun, et al., Chem. Commun. 56 (2020) 2723–2726.
[9] G. Begum, W.B. Goodwin, B.M. deGlee, et al., J. Mat. Chem. B 3 (2015) 5232–5240.
[10] Z. Zhao, T. Lin, W. Liu, et al., Spectrochim. Acta A Mol. Biomol. Spectrosc. 219 (2019) 240–247.
[11] Y. Zhang, J. Ge, Z. Liu, ACS Catal. 5 (2015) 4503–4513.
[12] J. Wu, S. Li, H. Wei, Chem. Commun. 54 (2018) 6520–6530.
[13] M. Liu, Z. Li, Y. Li, et al., Chin. Chem. Lett. 30 (2019) 1009–1012.
[14] R. Qu, L. Shen, A. Qu, et al., ACS Appl. Mat. Interfaces 7 (2015) 16694–16705.
[15] Y.C. Lee, M.I. Kim, M.A. Woo, et al., Biosens. Bioelectron. 42 (2013) 373–378.
[16] L. Li, S.Y. Sun, R. Lyu, et al., Chem. J. Chin. Univ.-Chin. 42 (2021) 803–810.
[17] A.J. Patil, E. Muthusamy, S. Mann, J. Mat. Chem. 15 (2005) 3838–3843.
[18] K.K.R. Datta, A. Achari, M. Eswaramoorthy, J. Mat. Chem. A 1 (2013) 6707.
[19] O.P. Setter, E. Segal, Nanoscale 12 (2020) 23444–23460.
[20] Y.F. Wei, P. Yuan, D. Liu, et al., Chem. Commun. 55 (2019) 2110–2113.
[21] L.T. Nguyen, K.L. Yang, Enzyme Microb. Technol. 100 (2017) 52–59.
[22] K. Carrado, L. Xu, R. Csencsits, J. Muntean, Chem. Mater. 13 (2001) 3766–3773.
[23] M. Liu, J. Mou, X. Xu, et al., Talanta 220 (2020) 121374.
[24] X. Peng, G. Wan, L. Wu, et al., Sens. Actuators B: Chem. 257 (2018) 166–177.
[25] X. Li, X. Yang, X. Cheng, et al., J. Colloid. Interface Sci. 570 (2020) 300–311.
[26] C. Lin, Y. Du, S. Wang, et al., Mater. Sci. Eng. C: Mater. Biol. Appl. 118 (2021) 111511.